



Open Access

ORIGINAL ARTICLE

Male Infertility

# Novel biallelic *HFM1* variants cause severe oligozoospermia with favorable intracytoplasmic sperm injection outcome

Liu Liu<sup>1,2,\*</sup>, Yi-Ling Zhou<sup>1,\*</sup>, Wei-Dong Tian<sup>2</sup>, Feng Jiang<sup>1,3</sup>, Jia-Xiong Wang<sup>4</sup>, Feng Zhang<sup>5,6</sup>, Chun-Yu Liu<sup>5,6</sup>, Hong Zhu<sup>1</sup>

Male factors contribute to 50% of infertility cases, with 20%–30% of cases being solely attributed to male infertility. Helicase for meiosis 1 (*HFM1*) plays a crucial role in ensuring proper crossover formation and synapsis of homologous chromosomes during meiosis, an essential process in gametogenesis. *HFM1* gene mutations are associated with male infertility, particularly in cases of non-obstructive azoospermia and severe oligozoospermia. However, the effects of intracytoplasmic sperm injection (ICSI) in *HFM1*-related infertility cases remain inadequately explored. This study identified novel biallelic *HFM1* variants through whole-exome sequencing (WES) in a Chinese patient with severe oligozoospermia, which was confirmed by Sanger sequencing. The pathogenicity of these variants was assessed using real-time quantitative polymerase chain reaction (RT-qPCR) and immunoblotting, which revealed a significant reduction in *HFM1* mRNA and protein levels in spermatozoa compared to those in a healthy control. Transmission electron microscopy revealed morphological abnormalities in sperm cells, including defects in the head and flagellum. Despite these abnormalities, ICSI treatment resulted in a favorable fertility outcome for the patient, indicating that assisted reproductive techniques (ART) can be effective in managing *HFM1*-related male infertility. These findings offer valuable insights into the management of such cases.

*Asian Journal of Andrology* (2025) 27, 1–6; doi: 10.4103/aja20259; published online: 02 May 2025

**Keywords:** *HFM1*; ICSI; male infertility; oligozoospermia

## INTRODUCTION

Infertility is defined as the inability of a couple to conceive after at least 1 year of regular, unprotected sexual activity.<sup>1</sup> This condition is a major concern in reproductive health, affecting millions of couples globally. Notably, male factors contribute to 50% of all infertility cases, with 20%–30% attributed solely to male infertility.<sup>1</sup> Among the various causes of male infertility, issues related to sperm count, motility, and morphology are particularly significant. Oligozoospermia, characterized by a low sperm count, and azoospermia, in which no sperms are present in the ejaculate, are prevalent conditions that substantially decrease the likelihood of natural conception.<sup>2</sup> Additionally, asthenozoospermia, characterized by reduced sperm motility, and teratozoospermia, involving abnormal sperm morphology, also contribute to impaired fertility.<sup>3–5</sup>

Genetic factors are increasingly recognized as key contributors to abnormal spermatogenesis.<sup>2,6–14</sup> A growing body of evidence suggests that specific gene mutations or chromosomal abnormalities can disrupt various stages of spermatogenesis, leading to reduced sperm count, impaired motility, and abnormal morphology. For example,

Y chromosome microdeletions and mutations in spermatogenesis-associated genes have been frequently linked to oligozoospermia and azoospermia.<sup>2</sup> Similarly, genetic abnormalities can affect sperm motility and morphology, contributing to asthenozoospermia and teratozoospermia.<sup>2</sup> Despite these insights, the genetic basis of male infertility remains incompletely understood, underscoring the need for further research to identify additional genetic factors involved in these conditions. Meiosis is a specialized cell division process that produces gametes by halving the chromosome number, ensuring gametes possess the correct chromosomal complement required for reproduction. Helicase for meiosis 1 (*HFM1*) plays a crucial role in meiosis, as it is essential for crossover formation and complete synapsis of homologous chromosomes.<sup>15–18</sup> Structurally, the *HFM1* gene consists of 39 exons and is located on human chromosome 1p22.<sup>19</sup> According to the Human Protein Atlas database, *HFM1* exhibits tissue-enhanced expression in the human testis and pituitary gland. Alterations in the *HFM1* gene have been linked to male infertility, particularly in cases of non-obstructive azoospermia and severe oligozoospermia.<sup>16,20–24</sup> However, the outcomes of intracytoplasmic

<sup>1</sup>Obstetrics and Gynecology Hospital, Fudan University, Shanghai 200011, China; <sup>2</sup>Department of Computational Biology, School of Life Sciences, Fudan University, Shanghai 200438, China; <sup>3</sup>Shanghai JIAI Genetics and IVF Institute-China USA Center, Shanghai 200011, China; <sup>4</sup>Center for Reproduction and Genetics, Suzhou Hospital Affiliated to Nanjing Medical University, Suzhou 215002, China; <sup>5</sup>Soong Ching Ling Institute of Maternity and Child Health, International Peace Maternity and Child Health Hospital, Shanghai Jiao Tong University School of Medicine, Shanghai 200030, China; <sup>6</sup>Shanghai Key Laboratory of Embryo Original Diseases, Shanghai 200030, China.

\*These authors contributed equally to this work.

Correspondence: Dr. CY Liu (liuchunyu@shsmu.edu.cn) or Dr. H Zhu (zhuhong7687@fckyy.org.cn)

Received: 19 September 2024; Accepted: 14 February 2025

sperm injection (ICSI) in patients with *HFM1*-related male infertility remain poorly documented.

In this study, we identified novel biallelic *HFM1* variants in a Chinese patient with severe oligozoospermia using whole-exome sequencing (WES). We evaluated the pathogenicity of these variants by comparing *HFM1* expression in the patient's sperm cells to that in a healthy control using real-time quantitative polymerase chain reaction (RT-qPCR) and western blot analysis. Furthermore, we documented the ICSI outcome for this patient with *HFM1* variants. Our findings provide clinical evidence supporting the use of assisted reproductive techniques (ART) to manage *HFM1*-related male infertility.

## PARTICIPANTS AND METHODS

### Ethical statement

The Ethics Committee of the Human Sperm Bank of Fudan University (Shanghai, China) approved this study (Approval No. 2019-05). Written informed consent was obtained from all participants prior to participation.

### Participants

A 34-year-old Chinese male with severe oligozoospermia was enrolled at the Obstetrics and Gynecology Hospital (Shanghai, China). The couple had been attempting to conceive for over a year without success. Physical examination revealed normal secondary sexual characteristics, with bilateral testicular volumes estimated at approximately 12 ml each. Hormonal analysis showed generally normal levels of sex hormones, including follicle-stimulating hormone (FSH; 7.60 mIU ml<sup>-1</sup>; reference range: 1.27–19.26 mIU ml<sup>-1</sup>), luteinizing hormone (LH; 6.63 mIU ml<sup>-1</sup>; reference range: 1.24–8.62 mIU ml<sup>-1</sup>), prolactin (PRL; 198.10 mIU l<sup>-1</sup>; reference range: 55.97–278.36 mIU l<sup>-1</sup>), testosterone (T; 8.15 nmol l<sup>-1</sup>; reference range: 6.07–27.1 nmol l<sup>-1</sup>), and estradiol (E2; 180.00 pmol l<sup>-1</sup>; reference range: <73.40–172.49 pmol l<sup>-1</sup>) which was slightly elevated above the reference range. Chromosomal karyotyping confirmed a 46,XY male. Additionally, tests for azoospermia factor (AZF) microdeletions, including AZFa, AZFb, and AZFc, detected no abnormalities on the Y chromosome.

For comparison, spermatozoa from a healthy donor recruited from the Human Sperm Bank of Fudan University was used as control sample.

### Semen analysis and sperm morphology assessment

Fresh semen samples from the patient were collected through masturbation after 2–7 days of sexual abstinence, following the 5<sup>th</sup> edition of the World Health Organization (WHO) guidelines.<sup>25</sup> Semen analyses were conducted three times using separate samples, and sperm morphology was assessed from a sample obtained after a 5-day abstinence period. Sperm concentration, total sperm count, and progressive motility rate (PR%) were measured using computer-aided sperm analysis (CASA; SCA<sup>®</sup> System, Hamilton Thorne Inc., Barcelona, Spain) after liquefaction. Makler<sup>®</sup> 0.01 mm deep semen counting chamber (68052-01; Sefi Medical Instruments, Haifa, Israel) was used under a phase-contrast microscope to count sperm at low concentrations (2 × 10<sup>6</sup> ml<sup>-1</sup>). Sperm morphology was evaluated through hematoxylin and eosin (H&E) staining, with at least 200 spermatozoa examined to calculate the percentage of morphologically abnormal sperm.

### WES and bioinformatics analysis

Genomic DNA was extracted from the patient's peripheral blood using a Magnetic Blood Genomic DNA Kit (DP329; Tiangen Biotech Co., Ltd., Beijing, China) according to the manufacturer's protocol. Whole-exome

capture was conducted with a TargetSeq One Enrichment Kit V2 Plus (iGeneTech, Beijing, China), and WES was performed on the Illumina NovaSeq 6000 system (Illumina, San Diego, CA, USA). Fastp was used to filter raw reads and remove low-quality sequences.<sup>26</sup> The cleaned reads were aligned to the human reference genome (GRCh37/hg19) using the Burrows–Wheeler Aligner (BWA).<sup>27</sup> Single-nucleotide variants (SNVs) and insertion/deletion mutations (InDels) were identified using the Genome Analysis Toolkit (GATK),<sup>28</sup> and the Ensembl Variant Effect Predictor (VEP) was employed for variant annotation.<sup>29</sup>

Variants were filtered based on allele frequencies obtained from public databases, including the Genome Aggregation Database (gnomAD) and the 1000 Genomes Project, excluding variants with an allele frequency above 1%. We prioritized rare variants with potential pathogenic effect, including loss-of-function (LoF) mutations (nonsense, frameshift, canonical splice site, and start-loss variants) and missense variants predicted to be deleterious by *in silico* tools. Additionally, variants in X-linked genes and biallelic mutations were selected for further analysis.

### Sanger sequencing

Blood samples were collected from the patient and his parents, and genomic DNA was extracted from all samples. Potential variants in the *HFM1* gene were amplified using primers listed in **Supplementary Table 1**. The presence of these variants was subsequently confirmed in each sample through Sanger sequencing.

### RT-qPCR

For RT-qPCR, total RNA was extracted from human spermatozoa using a Allprep DNA/RNA/Protein Mini Kit (QIAGEN, Hilden, Germany). Approximately 500 ng of RNA was used for complementary DNA (cDNA) synthesis with the Hiscript II Q RT SuperMix for RT-qPCR (Vazyme, Nanjing, China). The primers were designed and validated using the PrimerBank tool (<https://pga.mgh.harvard.edu/primerbank/index.html>) provided by Harvard University. For *HFM1* (PrimerBank ID: 130484566c1), the forward primer for cDNA amplification was located at positions 545–567 of transcript NM\_001017975, and the reverse primer was located at positions 686–706 of transcript NM\_001017975. For glyceraldehyde-3-phosphate dehydrogenase (*GAPDH*; PrimerBank ID: 378404907c1), the forward primer was located at positions 108–128 of transcript NM\_001256799, and the reverse primer was located at positions 282–304 of transcript NM\_001256799. RT-qPCR was performed on a CFX Connect<sup>™</sup> Real-Time PCR Detection System using the AceQ qPCR SYBR Green Master Mix (Vazyme). Each assay was conducted in triplicate for each sample, with the human *GAPDH* gene as an internal control. Data analysis was performed using the 2<sup>-ΔΔCt</sup> method. The RT-qPCR primers used are detailed in **Supplementary Table 2**.

### Electron microscopy analysis

For transmission electron microscopy (TEM), semen samples were fixed in 2.5% glutaraldehyde. Following fixation, the samples were rinsed three times with 0.1 mol l<sup>-1</sup> phosphate buffer (PB, containing dibasic sodium phosphate [Na<sub>2</sub>HPO<sub>4</sub>], sodium dihydrogen phosphate [NaH<sub>2</sub>PO<sub>4</sub>], and sodium chloride [NaCl], pH 7.4) and post-fixed in 1% osmium tetroxide in 0.1 mol l<sup>-1</sup> PB for 1–1.5 h at 4°C. The samples were then subjected to a stepwise dehydration process using ethanol at increasing concentrations (50%, 70%, 90%, and 100%), followed by 100% acetone. After dehydration, the samples were embedded in Epon 812 resin (90529-77-4; SPI, West Chester, PA, USA) and allowed to polymerize overnight at 37°C. They were subsequently placed in a thermostat at 37°C, 45°C, and 65°C for 12 h each. Ultrathin sections

(70 nm thick) were obtained using an ultramicrotome, stained with 4% uranyl acetate and lead citrate, and examined with a TEM (TECNAI-10; Philips, Eindhoven, the Netherlands) operating at an accelerating voltage of 80 kV. Images were captured for analysis.

### Western blot analysis

Proteins from human spermatozoa were extracted using a Allprep DNA/RNA/Protein Mini Kit (QIAGEN). The extracted proteins were mixed with 5× Protein Loading Dye (C508320-0001; Sangon Biotech, Shanghai, China) in a 4:1 volume ratio and heated at 95°C for 10–15 min. The lysates were separated via 10% sodium dodecyl sulfate-polyacrylamide gel electrophoresis (SDS-PAGE) at a constant voltage of 120 V for 90 min. Proteins were then transferred onto a polyvinylidene difluoride (PVDF) membrane (Millipore, Billerica, MA, USA) at a constant current of 300 mA for 60 min.

For western blotting, membranes were blocked with 5% non-fat milk in Tris-buffered saline containing 0.1% Tween-20 (TBST) for 1 h at room temperature. They were then incubated overnight at 4°C with primary antibodies: anti-HFM1 (PA5-83278, diluted 1:1000; Invitrogen, Carlsbad, CA, USA) or horseradish peroxidase (HRP)-conjugated  $\beta$ -actin (HRP-60008, diluted 1:3000; Proteintech, Chicago, IL, USA). After three washes with TBST, membranes were incubated with an HRP-conjugated anti-rabbit IgG secondary antibody (BF03008, diluted 1:3000; Biodragon, Suzhou, China) for 1 h at room temperature. Following another three TBST washes, immunoreactive protein bands were visualized using the Chemistar™ High-Sig ECL Western Blotting Substrate (Tanon, Shanghai, China) and imaged with a Tanon 5200 imaging system.  $\beta$ -actin served as the internal control.

### Statistical analyses

Data in this study underwent comparisons utilizing two-tailed unpaired Student's *t*-test, and  $P < 0.05$  was considered statistically significant.

## RESULTS

### Phenotype of sperm

H&E staining was used to assess sperm morphology. Compared to sperm from a control individual, the patient's sperm displayed significant morphological abnormalities in both the head and flagellum (Figure 1). Statistical analysis revealed higher rates of head defects, such as vacuolated heads and small acrosomes, as well as tail defects, including absent, short, and coiled flagella, in the patient's sperm cells (Table 1).

Further ultrastructural analysis was performed using TEM. Figure 2 shows that the core axoneme microtubule structure in

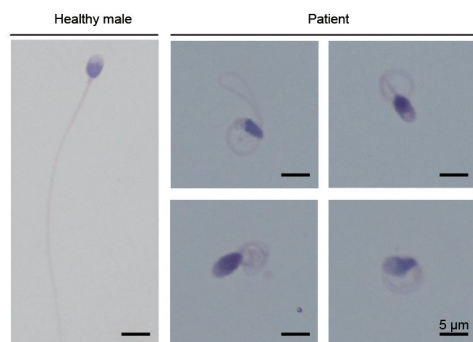


**Figure 1:** Sperm morphology analysis using H&E staining. H&E staining of spermatozoa from the patient displayed significant morphological abnormalities in both the head and flagellum compared with the normal spermatozoa from a healthy control. Scale bars = 5  $\mu$ m. H&E: hematoxylin and eosin.

sperm flagella from a healthy individual displayed the typical “9 + 2” arrangement, with nine peripheral microtubule doublets surrounding a central pair. In contrast, cross-sectional views of the patient's sperm flagella revealed the absence of central microtubules and disruption in the organization of the peripheral microtubule doublets. Additionally, the patient's sperm heads exhibited marked abnormalities compared to those of the control (Figure 2).

### Identification of novel biallelic HFM1 variants

WES was conducted to identify mutations associated with the patient's severe oligozoospermia. The analysis identified biallelic variants in the HFM1 gene: a C-to-T substitution at position 803 (c.803C>T), causing a

**Table 1: Semen characteristics and sperm morphology in the patient with HFM1 variants**

Characteristic	Patient	Reference
Semen parameter (mean $\pm$ s.d.)		
Semen volume (ml)	1.6 $\pm$ 0.6	1.5 <sup>a</sup>
Sperm concentration ( $\times 10^6$ ml <sup>-1</sup> )	4.5 $\pm$ 1.9	15.0 <sup>a</sup>
Total sperm count ( $\times 10^6$ per ejaculation)	6.5 $\pm$ 2.2	39.0 <sup>a</sup>
Progressive motility (%)	18.9 $\pm$ 6.8	32.0 <sup>a</sup>
Sperm morphology (%)		
Absent flagella	7.0	5.0 <sup>b</sup>
Short flagella	21.0	1.0 <sup>b</sup>
Coiled flagella	50.5	17.0 <sup>b</sup>
Angulation	2.5	13.0 <sup>b</sup>
Pyriform	4.0	1.0 <sup>c</sup>
Vacuolated	29.5	12.5 <sup>c</sup>
Small acrosome	23.5	7.5 <sup>c</sup>

<sup>a</sup>Reference criteria according to the 5<sup>th</sup> edition of the WHO guidelines.<sup>25</sup> <sup>b</sup>Reference criteria according to the distribution range of morphologically normal spermatozoa observed in 926 fertile individuals.<sup>37</sup> <sup>c</sup>Analyzed from more than 200 sperm cells from a healthy male donor recruited from the Human Sperm Bank of Fudan University. s.d.: standard deviation; WHO: World Health Organization; HFM1: helicase for meiosis 1

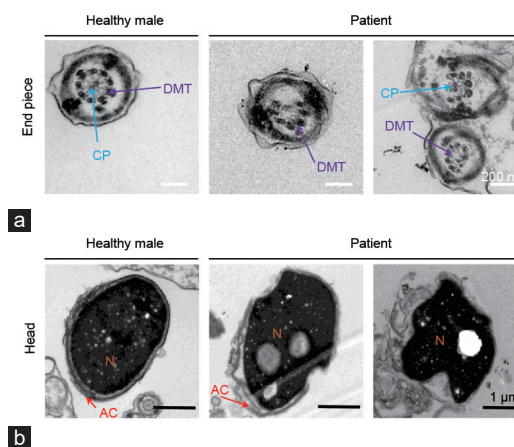


**Figure 2:** Transmission electron microscopy (TEM) of sperm flagella and heads. (a) Representative TEM image of the sperm flagellum end piece from a healthy male and the patient. The normal sperm showed the typical “9 + 2” microtubule arrangement (nine peripheral microtubule doublets and a pair of central microtubules), whereas the sperm from the patient showed the absence of central microtubules and disorganized peripheral microtubule doublets. Scale bars = 200 nm. CP: central pair apparatus (blue arrows); DMT: doublet microtubule (purple arrows). (b) Representative TEM image of the sperm head from a healthy male and the patient. The normal sperm showed normal nuclear shape and acrosome structure; whereas the sperm head from the patient showed clear abnormalities, including altered nuclear shape and abnormal acrosome structures. Scale bars = 1  $\mu$ m. N: nucleus; AC: acrosome (red arrows).

proline-to-leucine change at position 268 (p.Pro268Leu), and a second C-to-T substitution at position 2011 (c.2011C>T), introducing an early stop codon at position 671 (p.Arg671\*). Sanger sequencing of DNA samples from the patient and his parents confirmed the presence of these variants. The c.803C>T variant was inherited from the father, while the c.2011C>T variant was inherited from the mother, following an autosomal recessive inheritance pattern (Figure 3). This finding underscores the genetic basis of the patient's infertility.

**Interpretation of novel HFM1 variants**

The analysis identified two compound heterozygous deleterious variants in the HFM1 gene in a Chinese male with severe oligozoospermia: p.Pro268Leu and p.Arg671\*. The p.Arg671\* variant is a stop-gain mutation, expected to result in early termination of protein synthesis. This truncation likely leads to the loss of crucial functional domains of the HFM1 protein, as multiple LoF variants downstream of this site have been reported in male infertility patients,<sup>16,23</sup> highlighting the importance of the protein segment beyond this point. The allele frequency of p.Arg671\* is extremely low in the human population (0.000057 in East Asians in gnomAD, 0 in all individuals in the 1000 Genomes Project, and 0.000004 in all individuals in gnomAD), with no homozygous occurrences reported, suggesting a strong association with its deleterious effect.

The other variant, p.Pro268Leu, is a missense mutation. Several *in silico* tools, including SIFT, PolyPhen-2, MutationTaster, CADD\_phred, scSNV-ADA, and scSNV-RE, predict this variant to be deleterious. It also has a very low allele frequency in the human population (0 in East Asians in gnomAD, 0.000200 in all individuals in the 1000 Genomes Project, and 0.000045 in all individuals in gnomAD), with no homozygous cases reported. The consensus across various predictive algorithms and its low population frequency further supports its potential pathogenicity.

These results suggest that the p.Arg671\* and p.Pro268Leu variants contribute to the patient's infertility phenotype. The premature termination caused by p.Arg671\* and the deleterious missense change in p.Pro268Leu likely impair critical functions of the HFM1 protein, disrupting spermatogenesis and leading to the clinical presentation of severe oligozoospermia.

**Effects of identified variants on HFM1 expression**

RT-qPCR analysis revealed a significant reduction ( $P = 0.0007$ ) in HFM1 mRNA levels in the spermatozoa of the patient compared

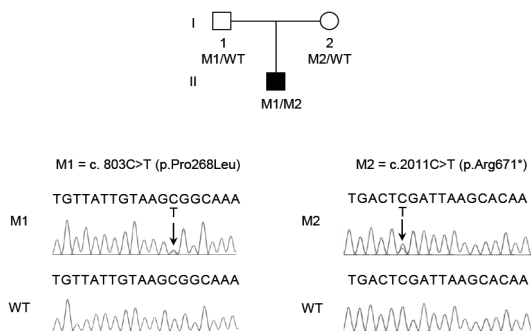


**Figure 3:** Identification of novel biallelic HFM1 variants in a severe oligozoospermia patient. Sanger sequencing results validated two heterozygous variants in the HFM1 gene: M1 = NM\_001017975:c.803C>T (p.Pro268Leu) and M2 = NM\_001017975:c.2011C>T (p.Arg671\*). The c.803C>T variant was inherited from the father, and the c.2011C>T variant was inherited from the mother. This supports an autosomal recessive inheritance pattern. HFM1: helicase for meiosis 1; M1: mutation 1; M2: mutation 2; WT: wild type.

to those of a healthy control (Figure 4a). This decrease in HFM1 expression suggests that the identified variants, p.Pro268Leu and p.Arg671\*, negatively affect the transcription or stability of the HFM1 mRNA, potentially contributing to the patient's infertility phenotype. Furthermore, immunoblotting assay demonstrated a marked reduction in HFM1 protein levels in the patient's sperm cells, with only a faint band detected compared to the healthy control (Figure 4b). These results collectively highlight the substantially reduced HFM1 expression in spermatozoa from a man harboring HFM1 variants, emphasizing the functional impact of these genetic alterations.

**Outcome of ICSI**

We present a summary of the clinical results from ICSI procedures, using spermatozoa from the patient with oligozoospermia and HFM1 variants (Table 2). The patient's female partner, 35 years old, had normal ovarian function and a normal chromosome karyotype. They underwent two ICSI cycles, with 10 oocytes injected, of which 7 achieved normal fertilization, resulting in a fertilization rate of 70.0%. Six transferable embryos were formed, yielding a transferable embryo rate of 85.7%. Three embryo transfer cycles were performed, with a total of 4 embryos transferred, leading to an implantation rate of 25.0%. A clinical pregnancy was achieved, resulting in one live birth, corresponding to a pregnancy and live birth rate per transfer

**Table 2: Clinical outcomes of ICSI using spermatozoa from the patient with HFM1 variants**

Clinical characteristic	Value
Male age (year)	34
Female age (year)	35
ICSI cycles (n)	2
Injected oocytes (n)	10
2PN zygotes (n)	7
Normal fertilization rate (%)	70.0
Transferable embryos (n)	6
Transferable embryo rate (%)	85.7
Embryo transfer cycles (n)	3
Transferred embryos (n)	4
Implantation rate (%)	25.0
Clinical pregnancy (n)	1
Clinical pregnancy rate per transfer cycle (%)	33.3
Live birth (n)	1
Live birth rate per transfer cycle (%)	33.3

ICSI: intracytoplasmic sperm injection; 2PN: 2 pronuclear; HFM1: helicase for meiosis 1

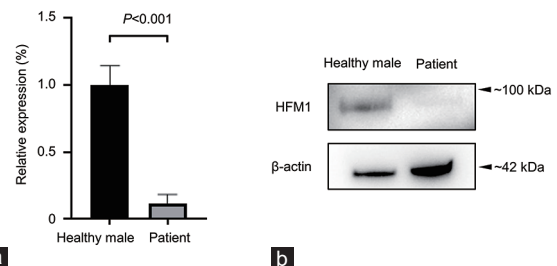


**Figure 4:** Impact of the identified HFM1 variants on gene expression. (a) RT-qPCR analysis revealed a significant reduction in HFM1 mRNA levels in the spermatozoa of the patient compared to those of a healthy control. (b) Western blot analysis demonstrated reduced HFM1 protein levels in the spermatozoa of the patient compared to those of a healthy control. This further confirms the impact of the identified variants on HFM1 expression. HFM1: helicase for meiosis 1; RT-qPCR: real-time quantitative polymerase chain reaction.

cycle of 33.3%. These results demonstrate that despite the presence of deleterious *HFM1* variants, successful fertilization, transferable embryo formation, and live birth can be achieved through ICSI treatment. Our results highlight the potential of ART to overcome genetic infertility challenges in patients with *HFM1* deficiency.

## DISCUSSION

This study reports novel biallelic *HFM1* variants associated with severe oligozoospermia and demonstrates a successful ICSI outcome in a patient with *HFM1* deficiency, a result not previously documented. Our findings expand the understanding of genetic factors contributing to male infertility and highlight the effectiveness of ART in managing cases with *HFM1* deficiency.

*HFM1* is essential for the formation of crossovers and the complete synapsis of homologous chromosomes during meiosis, processes critical for producing viable gametes.<sup>15–18</sup> Previous studies have linked *HFM1* mutations to non-obstructive azoospermia and severe oligozoospermia, suggesting that disruptions in this gene impair meiotic progression and contribute to infertility.<sup>16,20–24</sup> In our study, we identified two novel variants: p.Arg671\*, a stop-gain mutation likely causing the loss of essential functional domains, and p.Pro268Leu, a missense mutation predicted to be potentially harmful by various *in silico* tools. The rarity of these variants in the general population, coupled with their predicted pathogenicity, highlights their potential role in disrupting spermatogenesis. The significant reduction in *HFM1* mRNA levels and the notable decrease in *HFM1* protein levels observed in the patient's spermatozoa underscore the deleterious impact of these variants. These findings align with the critical role of *HFM1* in meiosis, where its disruption can severely impair chromosomal synapsis and crossover formation, leading to spermatogenic failure and severe oligozoospermia.

The clinical success of ICSI in this patient is particularly significant. Despite the presence of harmful *HFM1* variants, the patient achieved a normal fertilization rate, a normal transferable embryo rate, and a clinical pregnancy that resulted in a live birth. Although data on ART outcomes in patients with *HFM1* mutations are limited,<sup>30,31</sup> our findings suggest that ICSI can be an effective treatment even in the presence of substantial genetic impairments affecting spermatogenesis. While previous studies have shown the success of ICSI in cases of male infertility due to other genetic abnormalities,<sup>14,32–36</sup> our study provides new evidence of successful ICSI outcome in a patient with *HFM1*-related infertility. This underscores the potential of ICSI as a viable treatment for patients with similar genetic profiles.

This study not only improves our understanding of the genetic factors involved in severe oligozoospermia, but also offers valuable evidence supporting the use of ICSI in patients with *HFM1*-related infertility. Identifying patients with specific genetic defects will play a crucial role in delivering personalized and effective ART treatments. Future research will further elucidate the genetic causes of male infertility and enable more precise therapeutic strategies.

## AUTHOR CONTRIBUTIONS

LL conducted the genetic data analysis and wrote the manuscript. YLZ performed the experimental work. FZ and WDT contributed to the study design. FJ collected, analyzed, and interpreted clinical data related to ICSI outcome. JXW conducted the sperm phenotype analysis. CYL designed the experiments and revised the manuscript. HZ collected the case data and performed the clinical phenotype analyses. All authors read and approved the final manuscript.

## COMPETING INTERESTS

All authors declare no competing interests.

## ACKNOWLEDGMENTS

This study was supported by the National Natural Science Foundation of China (No. 32288101, No. 32370654, No. 32100480, and No. 32200485) and Shanghai Municipal Science and Technology Major Project (No. 2017SHZDZX01).

Supplementary Information is linked to the online version of the paper on the *Asian Journal of Andrology* website.

## REFERENCES

- Vander Borgh M, Wyns C. Fertility and infertility: definition and epidemiology. *Clin Biochem* 2018; 62: 2–10.
- Cannarella R, Condorelli RA, Mongioi LM, La Vignera S, Calogero AE. Molecular biology of spermatogenesis: novel targets of apparently idiopathic male infertility. *Int J Mol Sci* 2020; 21: 1728.
- Coutton C, Escoffier J, Martinez G, Arnoult C, Ray PF. Teratozoospermia: spotlight on the main genetic actors in the human. *Hum Reprod Update* 2015; 21: 455–85.
- Lehti MS, Sironen A. Formation and function of sperm tail structures in association with sperm motility defects. *Biol Reprod* 2017; 97: 522–36.
- Zuccarello D, Ferlin A, Cazzadore C, Pepe A, Garolla A, *et al*. Mutations in dynein genes in patients affected by isolated non-syndromic asthenozoospermia. *Hum Reprod* 2008; 23: 1957–62.
- Oud MS, Volozonoka L, Smits RM, Vissers L, Ramos L, *et al*. A systematic review and standardized clinical validity assessment of male infertility genes. *Hum Reprod* 2019; 34: 932–41.
- Sudhakar DV, Shah R, Gajbhiye RK. Genetics of male infertility – present and future: a narrative review. *J Hum Reprod Sci* 2021; 14: 217–27.
- Krausz C. Editorial for the special issue on the molecular genetics of male infertility. *Hum Genet* 2021; 140: 1–5.
- Krausz C, Escamilla AR, Chianese C. Genetics of male infertility: from research to clinic. *Reproduction* 2015; 150: R159–74.
- Jiao SY, Yang YH, Chen SR. Molecular genetics of infertility: loss-of-function mutations in humans and corresponding knockout/mutated mice. *Hum Reprod Update* 2021; 27: 154–89.
- Liu L, Tang SY, Zhang F, Jiang F. A novel homozygous loss-of-function mutation in *RAD51AP2* induces male infertility with nonobstructive azoospermia. *Asian J Androl* 2023; 25: 435–7.
- Liu L, Yang J, Zhang WJ, Zhou YL, Zhao GJ, *et al*. The identification of *AMZ2* as a candidate causative gene in a severe teratozoospermia patient characterized by vacuolated spermatozoa. *Asian J Androl* 2024; 26: 107–11.
- Zhu X, Liu L, Tian S, Zhao G, Zhi E, *et al*. Deleterious variant in *FAM71D* cause male infertility with asthenoteratospermia. *Mol Genet Genomics* 2024; 299: 35.
- Gao Y, Liu L, Tian S, Liu C, Lv M, *et al*. Whole-exome sequencing identifies *ADGB* as a novel causative gene for male infertility in humans: from motility to fertilization. *Andrology* 2024. Doi: 10.1111/andr.13605. [Online ahead of print].
- Guiraldelli MF, Eyster C, Wilkerson JL, Dresser ME, Pezza RJ. Mouse *HFM1/Mer3* is required for crossover formation and complete synapsis of homologous chromosomes during meiosis. *PLoS Genet* 2013; 9: e1003383.
- Xie X, Murtaza G, Li Y, Zhou J, Ye J, *et al*. Biallelic *HFM1* variants cause non-obstructive azoospermia with meiotic arrest in humans by impairing crossover formation to varying degrees. *Hum Reprod* 2022; 37: 1664–77.
- Wang H, Zhong C, Yang R, Yin Y, Tan R, *et al*. *HFM1* participates in Golgi-associated spindle assembly and division in mouse oocyte meiosis. *Cell Death Dis* 2020; 11: 490.
- Zhong C, Wang H, Yuan X, He Y, Cong J, *et al*. The crucial role of *HFM1* in regulating FUS ubiquitination and localization for oocyte meiosis prophase I progression in mice. *Biol Res* 2024; 57: 36.
- Tanaka K, Miyamoto N, Shouguchi-Miyata J, Ikeda JE. *HFM1*, the human homologue of yeast Mer3, encodes a putative DNA helicase expressed specifically in germ-line cells. *DNA Seq* 2006; 17: 242–6.
- Kherraf ZE, Cazin C, Bouker A, Fourati Ben Mustapha S, Hennebicq S, *et al*. Whole-exome sequencing improves the diagnosis and care of men with non-obstructive azoospermia. *Am J Hum Genet* 2022; 109: 508–17.
- Yao L, Ge Y, Du T, Chen T, Ma J, *et al*. A novel splicing mutation in helicase for meiosis 1 leads to non-obstructive azoospermia. *J Assist Reprod Genet* 2023; 40: 2493–8.
- Saebnia N, Ebrahimzadeh-Vesal R, Haddad-Mashhadrizeh A, Gholampour-Faraji N, Schinzel A, *et al*. Identification of a new splice-acceptor mutation in *HFM1* and functional analysis through molecular docking in nonobstructive azoospermia. *J Assist Reprod Genet* 2022; 39: 1195–203.
- Tang D, Lv M, Gao Y, Cheng H, Li K, *et al*. Novel variants in helicase for meiosis 1 lead to male infertility due to non-obstructive azoospermia. *Reprod Biol Endocrinol* 2021; 19: 129.



- 24 Zhang W, Song X, Ni F, Cheng J, Wu BL, *et al*. Association analysis between *HFM1* variations and idiopathic azoospermia or severe oligozoospermia in Chinese men. *Sci China Life Sci* 2017; 60: 315–8.
- 25 Cooper TG, Noonan E, von Eckardstein S, Auger J, Baker HW, *et al*. World Health Organization reference values for human semen characteristics. *Hum Reprod Update* 2010; 16: 231–45.
- 26 Chen S, Zhou Y, Chen Y, Gu J. Fastp: an ultra-fast all-in-one FASTQ preprocessor. *Bioinformatics* 2018; 34: i884–90.
- 27 Li H, Durbin R. Fast and accurate long-read alignment with Burrows-Wheeler transform. *Bioinformatics* 2010; 26: 589–95.
- 28 McKenna A, Hanna M, Banks E, Sivachenko A, Cibulskis K, *et al*. The genome analysis toolkit: a MapReduce framework for analyzing next-generation DNA sequencing data. *Genome Res* 2010; 20: 1297–303.
- 29 McLaren W, Gil L, Hunt SE, Riat HS, Ritchie GR, *et al*. The ensembl variant effect predictor. *Genome Biol* 2016; 17: 122.
- 30 Tang F, Gao Y, Li K, Tang D, Hao Y, *et al*. Novel deleterious splicing variant in *HFM1* causes gametogenesis defect and recurrent implantation failure: concerning the risk of chromosomal abnormalities in embryos. *J Assist Reprod Genet* 2023; 40: 1689–702.
- 31 Yu L, Li M, Zhang H, He Q, Wan F, *et al*. Novel pathogenic splicing variants in helicase for meiosis 1 (*HFM1*) are associated with diminished ovarian reserve and poor pregnancy outcomes. *J Assist Reprod Genet* 2022; 39: 2135–41.
- 32 Liu C, Tu C, Wang L, Wu H, Houston BJ, *et al*. Deleterious variants in X-linked *CFAP47* induce asthenoteratozoospermia and primary male infertility. *Am J Hum Genet* 2021; 108: 309–23.
- 33 Meng GQ, Wang Y, Luo C, Tan YM, Li Y, *et al*. Bi-allelic variants in *DNAH3* cause male infertility with asthenoteratozoospermia in humans and mice. *Hum Reprod Open* 2024; 2024: hoae003.
- 34 Liu C, Shen Y, Shen Q, Zhang W, Wang J, *et al*. Novel mutations in X-linked, *USP26*-induced asthenoteratozoospermia and male infertility. *Cells* 2021; 10: 1594.
- 35 Tian S, Wang Z, Liu L, Zhou Y, Lv Y, *et al*. A homozygous frameshift mutation in *ADAD2* causes male infertility with spermatogenic impairments. *J Genet Genomics* 2023; 50: 284–8.
- 36 Liu C, Si W, Tu C, Tian S, He X, *et al*. Deficiency of primate-specific *SSX1* induced asthenoteratozoospermia in infertile men and cynomolgus monkey and tree shrew models. *Am J Hum Genet* 2023; 110: 516–30.
- 37 Auger J, Jouannet P, Eustache F. Another look at human sperm morphology. *Hum Reprod* 2016; 31: 10–23.

This is an open access journal, and articles are distributed under the terms of the Creative Commons Attribution-NonCommercial-ShareAlike 4.0 License, which allows others to remix, tweak, and build upon the work non-commercially, as long as appropriate credit is given and the new creations are licensed under the identical terms.

©The Author(s)(2025)

**Supplementary Table 1: Primers used for amplification and verification of helicase for meiosis 1 mutations**

<i>Primer names</i>	<i>Primer sequences (5'-3')</i>	<i>Temperature</i>
M1-F	TTGCCAAGAAATACCACTGA	52.5°C
M1-R	GTATTATGGGAACATCAGGAAG	
M2-F	ACTTAGCCAGGAGTGGTGTC	56°C
M2-R	CTTCCTGTCAAGCCAGTATG	

**Supplementary Table 2: Primers used for real-time quantitative polymerase chain reaction assay**

<i>Primer names</i>	<i>Primer sequences (5'-3')</i>	<i>Temperature</i>	<i>Product length</i>
H- <i>HFM1</i> -F	ATGAATTGGACTCTCACATTGGC	56°C	162 bp
H- <i>HFM1</i> -R	ACATGCCTTCTCCGATTCAG		
H- <i>GAPDH</i> -F	GGAGCGAGATCCCTCCAAAAT	60°C	197 bp
H- <i>GAPDH</i> -R	GGCTGTTGTCATACTTCTCATGG		

*HFM1*: helicase for meiosis 1